Al-Khwarizmi Engineering Journal

Al-Khwarizmi Engineering Journal, Vol. 9, No. 3, P.P. 80- 99 (2013)

# Pressure Control of Electro-Hydraulic Servovalve and Transmission Line Effect

**Jafar Mehdi Hassan*  Yiqin Xue**  Majid Ahmed Oleiwi***
Ahmed Fouad Mahdi******

*Department of Mechanical Engineering / University of Technology
**Institute of Mechanical Engineering / Cardiff School of Engineering /UK
*** Department of Control and System Engineering / University of Technology
**** Department of Automated Manufacturing Engineering / Al-Khawarizmi College of Engineering
*Emal: JafarMahdi1951@yahoo.com
**Emal: xue@cf.ac.uk
***Emal: moleiwi@yahoo.com
****Emal: afmkridi@hotmail.com

(Received 17 March 2013; accepted 31 October 2013)

## Abstract

The effected of the long transmission line (TL) between the actuator and the hydraulic control valve sometimes essentials. The study is concerned with modeling the TL which carries the oil from the electro-hydraulic servovalve to the actuator. The pressure value inside the TL has been controlled by the electro-hydraulic servovalve as a voltage supplied to the servovalve amplifier. The flow rate through the TL has been simulated by using the lumped π element electrical analogy method for laminar flow. The control voltage supplied to servovalve can be achieved by the direct using of the voltage function generator or indirect $C^{++}$ program connected to the *DAP-view* program built in the *DAP-card* data acquisition connected to *PC*, to control the value of pressure in a selected point in the TL. It has been found that the relation between the voltage value and the output flow rate from the servovalve in most of the path is a linear relation. The MATLAB *m-File* program is used to create a representation state of the mathematical model to find a good simulation for the experimental open loop control test.

***Keywords:*** *Electro-hydraulic servovalve, Twin flapper nozzle, Transmission Line effect, Open loop Pressure control, Voltage linearization Equation, DAP-view Data Acquisition.*

## 1. Introduction

Servovalves were developed to facilitate the adjustment of fluid flow based on changes in load motion. The twin nozzle flapper servo valve is a high quality parts combined from mechanical, electrical and hydraulic technology and has the advantages of large power ratio, fast response, and high level of control precision. It is widely used in industrial applications such as manufacturing systems, robotics, materials test machines, active suspension systems, flight simulation, injection moulding machines…etc. Hydraulic systems are also common in aircraft, where their high power-to-weight ratio and precise control make them an ideal choice for actuation of flight surfaces [1].

Although they are commonly placed as close as possible to the device to which they are supplying fluid in some applications, it is not possible to place servo valves close to the actuator due to the plant conditions. This is commonly seen in the steel rolling industry [2].

In the last decades, some researchers have published some works in the field of servo valves modeling.

Watton and Hawkley, (1996) an approach is developed by utilizing measurements of transient pressure and flow rate at the inlet and outlet of the line. A time series analysis technique is used in

such a way that the number of unknown coefficients to be estimated is minimized. For three different line configurations and a range of operating conditions there is an accurate prediction which is shown for three different line configurations and a range of operating conditions. The evaluation of just two transmission line functions then allows a simple model structure to be used for the simulation of fluid power circuits incorporating long lines [3].

Krus and Nyman (2000) have demonstrated how the actuation system control surfaces with transmission line can be simulated using a flight dynamics model of the aircraft coupled to a model of the actuation system. In this way, the system can then be optimized for certain flight condition by "test flying" the system. The distributed modeling approach used makes it possible to simulate this system faster than real time on a 650 MHz PC. This means that even system optimization can be performed in reasonable time [4].

Dong Zhu and Lu (2010) prove that the long pipeline in hydraulic system has some influence on system performances and causes the system to become unstable. They target a hydraulic servo system with long transmission line between hydraulic power supply and servovalve, a mathematical model considering pipeline effect established by means of the theories of transmission line dynamics and hydraulic control systems in which pipeline characteristics were depicted by lumped-parameter model. Dong used AMESim (a software for modeling, simulation and dynamic analysis of hydraulic and mechanical system based on bond graph and which is a production of imagine corporation of France) to simulate the impact on system dynamic behaviors which were investigated theoretically and the influences of pipeline structural parameters on hydraulic system dynamic characteristics were analyzed [5].

Yang and Moan (2011) studied a heaving-buoy wave energy converter equipped with hydraulic power take off. This wave energy converter system is divided into five subsystems: a heaving buoy, hydraulic pump, pipelines, non-return check valves and a hydraulic motor combined with an electric generator. A dynamic model was developed by considering the interactions between the subsystems in a state space form. The simulation results show that transmission line dynamics play a dominant role in the studied wave energy converter system. The length of the pipeline will not only affect the amplitude of the transient pressures but also affect the converted power transformed in the generator [6].

The purpose of this work is to study the control of pressure losses in the transmission lines of hydraulic system using a servovalve. A theoretical analyses and experimental test are used to perform the work by applying direct voltage to control the pressure in a specific point in TL.

The system's dynamic characteristics have been tested by using a PC (Personal Computer) equipped with a data acquisition processor (DAP-card). This will allow data based modeling to be carried out, allowing prediction of the system's response to a given control output.

## 2. System Description

### 2.1.1. System Hardware Description

As shown in Fig. 1, the pressure supply line delivers hydraulic fluid from big power unit supply to the test rig at a pressure up to 150bar. A variable pressure relief valve is installed in the rig so the desired pressure can be achieved on the rig as the researcher needs. There is a temperature sensor and flow meter on the supply line to the servovalve. The valve to be used is an Ultra servovalve from Moog, of type 4658-249-810, shown in Fig. 2; the valve consists of two-stage, nozzle/flapper, and dray torque motor unit.

Service port B (see Fig. 1) is blocked rather than feeding to the annulus side of the actuator as might be expected. The service port A is the exit to the servovalve, where the second flow meter and pressure transducer located. The servo and actuator are connected via a long transmission line. This line is expected to have an important input to the dynamic response of the system due to its considerable length. The actual actuator is fixed into a position - it cannot move. This is allowable because the system is used to provide adequate force to counteract roll bending under load (work roll bending system). The actual displacement of these actuators are small, and would ideally be zero. Hence, when modeling this system it considered reasonable to ignore the small actuator movements. The PC records the Data Acquisition Processor (DAP card), which is connected to the transducer display and amplifier units as shown in Fig. 1.

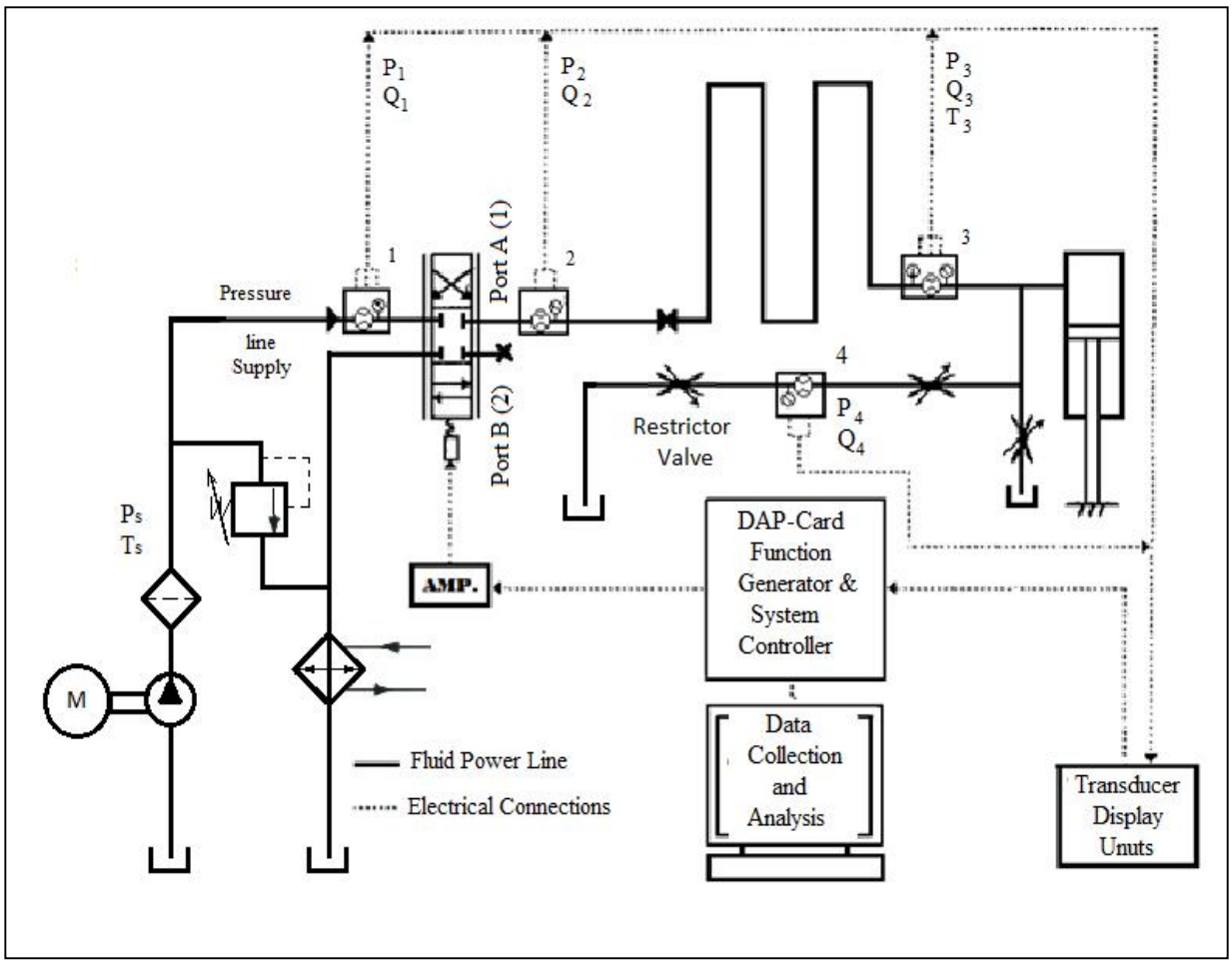


**Fig. 1. Schematic of System Set Up Cardiff University Laboratory.**

### 2.1.2. System Control Software Description

The DAP-card is connected to the PC and has its own operating system and it is provided with a program called DAP-view through which the control of the DAP-card is built. This program starts and stops collecting data, as well as outputting signals and logging every event. This project requires the use of custom written control commands, which will collect input signals to the card, process them in accordance with the desired control method, and pass them back to the DAP-view program to be sent to the equipment. Custom commands are written in $C^{++}$ language and have to be compiled and downloaded into the DAP-card. $C^{++}$ programs can only be changed by the PC, so any adjustments to the custom commands require the removal of previous custom commands and recompilation and installation on the DAP-card [7].

## 2.2. Servovalve Construction

The servovalve is an interface between low energy electrical signals and high-level hydraulic power. Servo valves are electrically operated proportional directional control valves. They are usually four port units which control the quantity of fluid they pass, as well as the direction. Most common servovalves are made in the form of a two-stage device [8].

### 2.2.1. First stage

The first stage contains a torque motor which operates an armature and this armature pivots a 'flapper' which is situated between two fixed nozzles. By applying a current to the torque motor, the armature is rotated, and this moves the flapper toward one nozzle, and away from the other. The flapper is located within the valve and hence is surrounded by hydraulic fluid. To keep

the torque motor free from oil, the flapper is

### 2.2.2. Second Stage

Second stage is typically a four-way spool valve that controls the fluid flow to two service ports. There is commonly a mechanical feedback system in the form of a feedback spring attached to the spool which acts to oppose the action of the torque motor on the flapper. See Fig. 2[8].

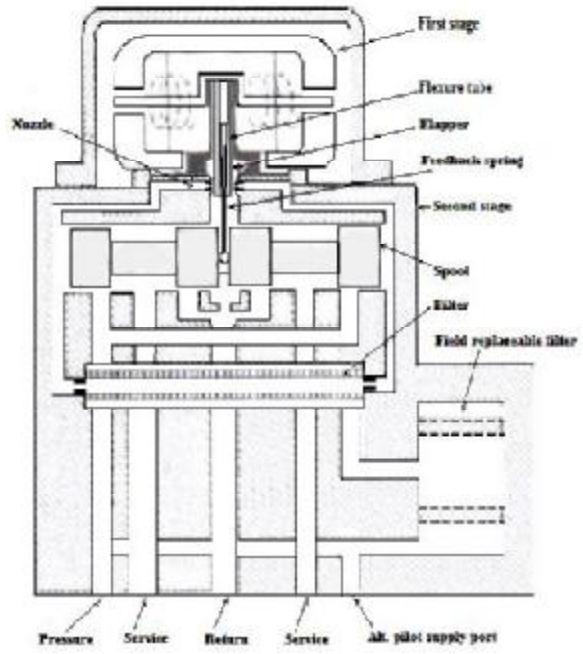


**Fig. 2 . Ultra /Moog servovalve, Type 4658 and its Cross Sectional View[9].**

## 2.3. Servovalve Modeling

### 2.3.1 Steady State Modeling of Servovalve

encased within a flexible 'flexure tube'[8].

When an electrical current is applied to the coils of the torque motor, a torque is generated on the armature. The armature and flapper are supported on the flexure tube or sleeve which separates the electro-magnetic and hydraulic parts of the valve which also provides a low friction pivot see Fig. 3. Four force components are considered in the torque motor. These are a positive function of the applied current and the rotation. These are a positive function of the applied current and the rotation. These forces are opposed by a torque from the stiffness of the flexure tube, and the net hydraulic force acting on the flapper element [9].

$$T = k_t\,\Delta i + k_m\theta - k_a\theta - (P_a - P_b)a_n r \quad \ldots(1)$$

The mechanical feedback element is one of the types of servovalve being considered. The torque of this feedback spring can be considered as follows for small values of θ:

$$T_f = k_f y(r + b), \quad y = x_s + (r + b)\theta \quad \& \quad x = r\theta \quad \ldots(2)$$

Atonement equation (2) in (1) gives the total torque on the torque motor Fig. 3, flapper and spring combination, noting that the torque is zero at steady state; the angle θ can be deduced [9]:

$$\theta = \frac{k_t\,\Delta i - a_n r(P_a - P_b) - k_f(r + b)x_s}{k_a - k_m + k_f(r + b)^2} \quad \ldots(3)$$

As can be seen from Fig. 4, there is a hydraulic 'bridge circuit' which is supplied with system pressure. A small amount of fluid can flow out through the fixed orifice and onward to the two variable orifices created by the nozzle/flapper interface, ultimately returning to the tank. Flapper/nozzles in conjunction with a pair of orifices used to generate a pressure difference by small movements of the flapper positioned midway between the nozzles, as shown in Fig. 4 [10].

The spool area and velocity are A, U respectively. Typically the nozzle diameter is dn= 0.5mm, the flapper clearance in the mid-position xnm= 0.03mm, and the orifice diameter do = 0.2mm. It is common for such a device to be used in servovalves as a mechanical feedback, the pressure difference generated being used to move the spool. It will be immediately clear from Fig. 4

that at the flapper mid position, often called the null position, the maximum leakage flow back to tank will exist, hence producing a small inherent power loss. As illustrating example, the flapper is moved to the left, by electromagnetic means then pressure P1 will increase and pressure P2 will decrease, thus providing a pressure difference across the spool which will then move unless restrained in some way. The flow loss and power loss will decrease as the flapper position is changed [10]. To analyze the flapper-nozzle bridge, the conventional restrictor flow equations are appropriate and given by:

$$Q_a = Q_x + a_s U, \quad a_{nx} = \pi d_n (x_{nm} - x), \qquad \ldots(4)$$

$$Q_b = Q_y - a_s U, \quad a_{ny} = \pi d_n (x_{nm} + x); \qquad \ldots(5)$$

$$Q_a = C_{qo} a_o \sqrt{\frac{2(P_s - P_a)}{\rho}}, \quad Q_b = C_{qo} a_o \sqrt{\frac{2(P_s - P_b)}{\rho}}; \qquad \ldots(6)$$

$$Q_x = C_{qn} a_{nx} \sqrt{\frac{2P_a}{\rho}}, \quad Q_y = C_{qn} a_{ny} \sqrt{\frac{2P_b}{\rho}}; \qquad \ldots(7)$$

At condition in which the spool motion is negligible, the steady-state performance of the double flapper-nozzle amplifier may be derived from equating Qa = Qx and Qb = Qy. This gives:

$$\bar{P}_a = \frac{1}{1+Z(1-\bar{x})^2} = \frac{P_a}{P_s}, \quad \bar{P}_b = \frac{1}{1+Z(1+\bar{x})^2} = \frac{P_b}{P_s}, \quad \bar{x} = \frac{x}{x_{nm}}; \qquad \ldots(8)$$

$$Z = 16\left(\frac{C_{qn}}{C_{qo}}\right)^2 \left(\frac{d_n}{d_o}\right)^2 \left(\frac{x_{nm}}{d_o}\right)^2, \qquad \ldots(9)$$

Then the differential pressure is given by:

$$\bar{P}_a - \bar{P}_b = \frac{4Z\bar{x}}{[1 + Z(1+\bar{x})^2][1 + Z(1-\bar{x})^2]}, \qquad \ldots(10)$$

Considering the null condition where $\bar{x} = 0$ and $\bar{P}_a - \bar{P}_b = 0$; that leads to:

$$\bar{P}_a = \bar{P}_b = \frac{1}{(1+Z)} \qquad \ldots(11)$$

and the null gain condition is:

$$\frac{d(\bar{P}_a - \bar{P}_b)}{d\bar{x}} = \frac{4Z}{(1+Z)^2} \qquad \ldots(12)$$

Because flapper operation is designed to be around the central (null) position, the pressure difference generated may be simply written as:

$$(P_a - P_b) = \left(\frac{x}{x_{nm}}\right) P_s \qquad \ldots(13)$$

Spool displacement is then determined from the force balance across the spool which is dominated by the feedback wire force and the spool flow reaction force:

$$(\mathrm{P_a - P_b})\mathrm{a_s} = \mathrm{ky} + 2\mathrm{C_q^2 a_o \cos\theta [P_s - P_{Load}]}, \quad \text{and} \quad \mathrm{a_o = wx_s} \qquad \ldots(14)$$

$$\text{And:} \quad \mathrm{P_{load} = P_1 - P_2} \quad \& \quad \mathrm{P_s = P_1 + P_2}$$

Where, as will the spool end cross section area, the spool orifice area ao for rectangular ports have an area gradient *w.* by combining these equations then give the relationship between spool displacement and input current is as follows:

If:

$$\alpha = \frac{k(r+b)x_{nm}}{rP_s a_s}; \qquad \ldots(15)$$

$$\beta = k_a - k_m + k(r+b)^2 + \frac{a_n r^2 P_s}{x_{nm}} \qquad \ldots(16)$$

$$k_{fr} = 2C_q^2 w \cos\theta \, (P_s - P_{load}) \qquad \ldots(17)$$

Then:

$$x_s = \frac{(1-\alpha)k_t i}{\beta\frac{(k-k_{fr})x_{nm}}{rP_s a_s} + k(r+b)(1-\alpha)} \qquad \ldots(18)$$

The spool displacement will be proportional to input current provided that the denominator of Eq. (18) is positive. The flow reaction equivalent stiffness $k_{fr}$ will probably be much smaller than the wire stiffness *k*, so that the effect of load pressure difference $P_{load}$ may not present a problem. In practice, $\alpha << 1$ and can be neglected. Notice also that the destabilizing magnetic constant $-k_m$, the magnitude of which can be varied during manufacture, the process known as detuning. In particular, $\beta$ can be detuned to a very small value by magnetically increasing $k_m$ and Eq. (18) then becomes:

$$x_s \approx \frac{k_t i}{k(r+b)} \qquad \ldots(19)$$

The input electrical torque is balanced by the wire feedback torque because of spool position, and the flapper will return to its central position between the nozzles [10]. Clearly, for the same servovalve, the value of *k*, *r* and *b* constants the spool displacement which can be proportional to current is dominated.

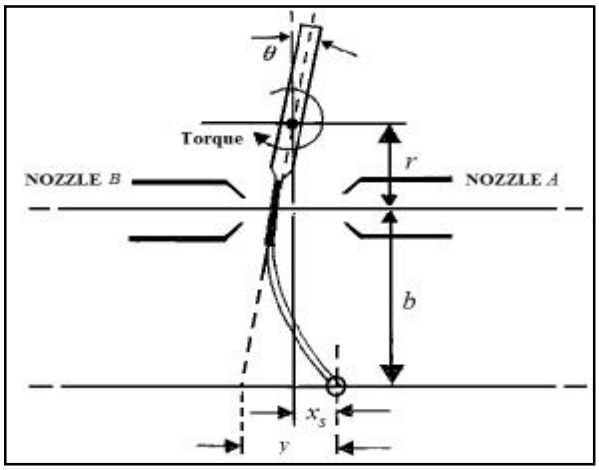


**Fig. 3. Feedback Spring Free Body Diagram [9].**

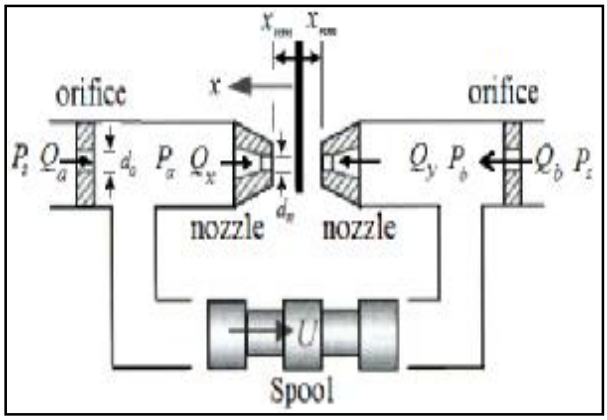


**Fig. 4. Schematic of a Double Flapper-Nozzle Amplifier used to Move A Spool [10].**

### 2.3.2 Dynamic Modeling of Servovalve

The steady state performance of the valve will need to be augmented by a model for the transient response, and also for the transient response of the fluid transmission line. This will allow predictive control to be used. For the servovalve that again requires a finite time to change its spool position in response to a change in applied current. The combination of these issues means that the design of both open-loop and closed-loop control systems should take into account these dynamic issues.

For the force-feedback type shown in Fig. 5, it is clear what components which contribute toward the overall dynamic performance. The use of a current-feedback servo-amplifier means that the current-buildup characteristic is extremely fast when compared with other elements of the servovalve.

The dynamic effect caused by the time required to generate the drive current can be ignored. However, there are effects produced from the flapper inertia and fluid viscosity [10].

The current-buildup and the dynamic torque equations will have the following types:

$$k_t i = (k_a - k_m)\theta + (P_a - P_b)a_n r + k[x_s + (r + b)\theta](r + b) + B_v \frac{d\theta}{dt} + J\frac{d^2\theta}{dt^2} \quad \ldots(20)$$

Apply the continuity equation on each side gives:

$$C_{qo}a_o\sqrt{\frac{2(P_s - P_a)}{\rho}} - C_{qn}a_{nx}\sqrt{\frac{2P_a}{\rho}} = +a_s\frac{dx_s}{dt} + \frac{V_a}{\beta}\frac{dP_a}{dt} \quad \ldots(21)$$

$$C_{qo}a_o\sqrt{\frac{2(P_s - P_b)}{\rho}} - C_{qn}a_{ny}\sqrt{\frac{2P_b}{\rho}} = -a_s\frac{dx_s}{dt} + \frac{V_b}{\beta}\frac{dP_b}{dt} \quad \ldots(22)$$

Where:

$$a_{nx} = \pi d_n(x_{nm} - x), \quad a_{ny} = \pi d_n(x_{nm} + x) \quad \& \quad x = r\theta$$

$V_a$ and $V_b$ are the internal, small volumes on either side of and within the flow resistance bridge.

The static force balance at the spool, including the flow reaction force, is now modified to include the dynamic flow reaction force, the spool viscous damping, and acceleration effects:

$$(P_a - P_b)a_s = k[x_s + (r + b)\theta] + 2C_q^2 w x_s \cos\theta[P_s - P_{load}] + \rho\, l\left(\frac{dQ_1}{dt} - \frac{dQ_2}{dt}\right) + B_s\frac{dx_s}{dt} + m\frac{d^2x_s}{dt} \quad \ldots(23)$$

Where:

$$Q_1 = C_q w x_s\sqrt{\frac{2(P_s - P_1)}{\rho}},$$

$$Q_2 = C_q w x_s\sqrt{\frac{2P_2}{\rho}} \quad \ldots(24a)$$

Obviously, the defining equations of servovalve are nonlinear, and the solution also requires the load specification so that the load pressure difference ($P_1$ - $P_2$) can be derived. Considering the equations presented, it will be seen that a valve dynamic performance depends not only on electrical-electromagnetic-geometry parameters but also on the load it supplied $P_{load}$ and, hence, on the load flow rate, the supply pressure $P_s$ , and the magnitude of the input current.

The tank (return line) pressure is usually neglected in comparison to the line pressures. The port opening area ($wx_s$) is proportional to spool displacement which is also proportional to the current applied to the electromagnetic first stage. Servovalve manufacturers also quote the rated flow at the valve rated current and with a valve pressure drop of 70*bar*, that is, the total pressure drop across both ports. Consequently the servovalve equations could be rewritten in the following form [10].

$$Q_1 = k_c i\sqrt{(P_s - P_1)} \quad \& \quad Q_2 = k_c i\sqrt{P_2} \qquad \ldots(24b)$$

From the previous equations and the contribution of dynamics behavior shown in Fig. 5, the amount of hydraulic fluid flow from the servovalve depends on the pressure and the current value coming to servovalve amplifier. In the steady state condition, both of the electromagnetic and mechanical properties are considered constant, as well as the effect of the amplifier, which converted the voltage value coming from the *DAP-view* programs to the servovalve amplifier. In other words, it can be considered that the hydraulic flow rate ($Q$) is a function of the voltage and the pressure as follows:

$$Q = f(v, P) \qquad \ldots(25)$$

At steady state operating condition ( $v_{ss}$, $P_{1ss}$, $P_{2ss}$, $Q_{1ss}$, $Q_{2ss}$), the first linear term of the *Taylor series* expansion for a nonlinear function will be employed. Consequently small changes in each parameter lead to:

$$\delta Q_1 = k_{v1}\delta v_{ss} - K_{p1}\,\delta P_1 \quad \& \quad \delta Q_2 = k_{v2}\delta v_{ss} + K_{p2}\,\delta P_2 \qquad \ldots(25a)$$

$$K_{v1} = \frac{\partial Q_1}{\partial v_{ss}} = K_f\sqrt{P_s - P_{1ss}} = \frac{Q_{1ss}}{v_{ss}} \qquad Flow\ Gain \qquad \ldots(25b)$$

$$K_{v2} = \frac{\partial Q_2}{\partial v_{ss}} = K_f\sqrt{P_{2ss}} = \frac{Q_{2ss}}{v_{ss}} \qquad Flow\ Gain \qquad \ldots(25c)$$

$$K_{p1} = \frac{\partial Q_1}{\partial P_1} = \frac{K_f v_{ss}}{2\sqrt{P_s - P_{1ss}}} = \frac{Q_{2ss}}{2(P_s - P_{1ss})} \qquad Pressure\ Coefficient \qquad \ldots(25d)$$

$$K_{p2} = \frac{\partial Q_2}{\partial P_2} = \frac{K_f v_{ss}}{2\sqrt{P_{2ss}}} = \frac{Q_{2ss}}{2(P_{2ss})} \qquad Pressure\ Coefficient \qquad \ldots(25e)$$

$$K_{vp} = \frac{\partial P}{\partial v_{ss}} = -\frac{\frac{\partial Q}{\partial v_{ss}}}{\frac{\partial Q}{\partial P}} = \frac{K_v}{K_p} = \frac{2(P_s - P_{1ss})}{v_{ss}} = \frac{2P_{2ss}}{v_{ss}}, Pressure\ sensivity \qquad \ldots(25f)$$

Also the servovalve equation could be written as:

$$Q_1 = k_c v\sqrt{(P_s - P_1)} \quad \& \quad Q_2 = k_c v\sqrt{P_2} \qquad \ldots(25g)$$

In this application, the singe action operation will be considered, so the port B (number *2* in previous equations) has been canceled, see Fig .1, thus, it is needed to consider the segment of the first port to find the value of flow gain and pressure coefficient equations (25b & 25d) at steady state condition.

Practically, the dynamic characteristic is often specified by the manufacturer as a frequency-response diagram for the spool position (input) and the flow rate (output) for a typical performance range.

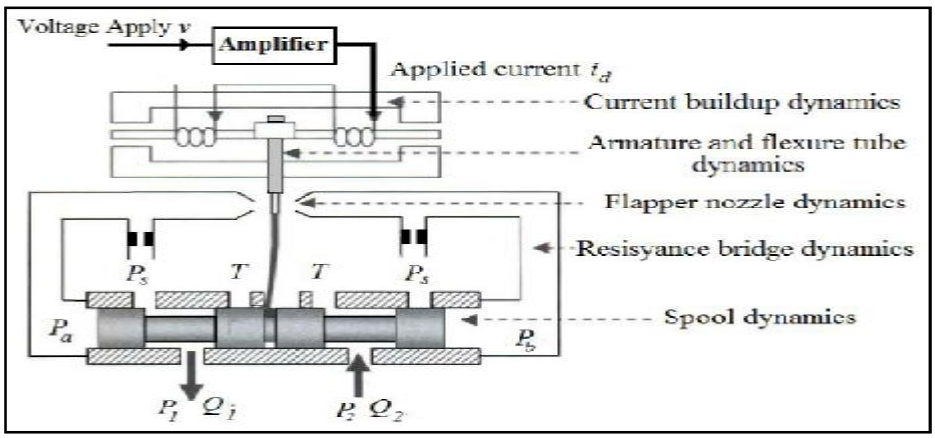

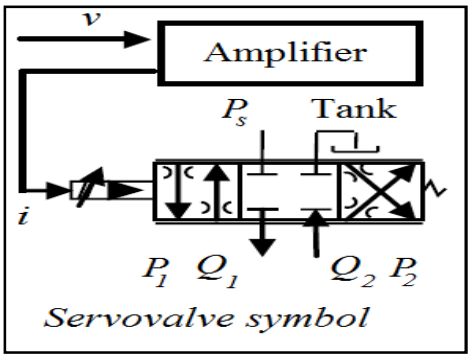


**Fig. 5. Contribution to Servovalve Dynamic Behavior [1] [10].**

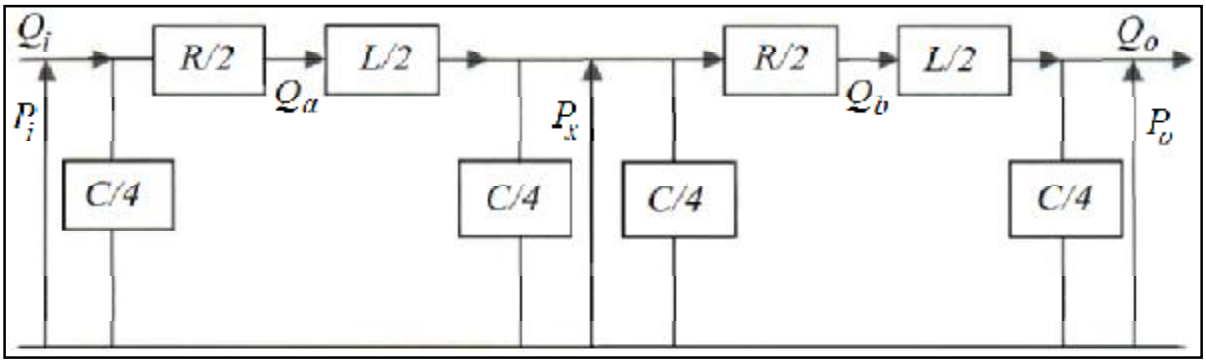


**Fig. 6. The Line Dynamics Approximation using Lumped π Elements For Laminar Mean Flow [4].**

## 2.4. Transmission Line Modeling

Hydraulic pipelines, when they are of significant length, they have an important effect upon the performance of many systems. The electrical analogy is a useful mechanism for understanding this approach [10]. Consider linear characteristics and a slug of fluid, ($a$) is cross sectional area and the length is ($l$ ).

**a. Fluid resistance**: The pressure drop ΔP, along the fluid element for laminar flow , is given by:

$$\Delta P = \frac{128\mu l}{\pi d^4} Q \quad \rightarrow \quad \Delta V_e = RI \qquad \ldots(26a)$$

Hydraulic resistance ⟶ Electrical resistance

**b. Fluid Compressibility:**

$$\Delta Q = \frac{V}{\beta}\frac{dP}{dt} \quad \rightarrow \quad \Delta I = C\frac{dV_e}{dt} \qquad \ldots(26b)$$

Fluid compressibility ⟶ Electrical capacitance

**c. Fluid Inertia:** The pressure drop that is due to fluid acceleration is given by:

$$\Delta Pa = \rho l a \frac{dU}{dt}, \quad \Delta P = \frac{\rho l}{a}\frac{dQ}{dt} \quad \rightarrow \quad \Delta V_e = E_i \frac{dI}{dt} \qquad \ldots(26c)$$

Fluid mechanical mass ⟶ Electrical inductance

$$Resistance \rightarrow R = \frac{128\mu l}{\pi d_i^4}, \; Inductance \rightarrow E_i = \frac{\rho l}{a} \; \& \; Capacitance \rightarrow C = \frac{V}{\beta} \qquad \ldots(26d)$$

If a system is expected to have a frequency component that is comparable with this frequency, line dynamics must be modeled with some accuracy. The issue is how to distribute *R*, *L* and *C* in the line and how many "*lumps*" should be used [10]. This work shows a two-lump approximation using a pair of π networks as shown in Fig. 6.

The set of equations using this approximation, and working from left to right, may then be written as follows:

$$Q_i - Q_a = \frac{C}{4}\frac{dP_i}{dt}, \quad Q_a - Q_b = \frac{C}{4}\frac{dP_x}{dt}, \quad Q_b - Q_o = \frac{C}{4}\frac{dP_o}{dt} \qquad \ldots(27a)$$

$$P_i - P_x = \frac{R}{2}Q_a + \frac{L}{2}\frac{dQ_a}{dt}, \quad P_x - P_o = \frac{R}{2}Q_b + \frac{L}{2}\frac{dQ_b}{dt} \qquad \ldots(26b)$$

These equations can be resolved when the input and the output pressure flow relationships

have been included to close the solution. So the pressure and flow meter sensors are needed in the test rig to record the overall pressure difference between the input and output for the transmission line, as shown in Fig. 1 and Fig. 7. This pressure difference can be used to calculate the losses that occur in the TL and the fittings which include such as bends, elbows, restricted valves and sudden expansion or contraction and other minor losses.

To solve the previous equations, it is necessary to make some practical experiences to achieve steady state condition, through collecting this kind of data. The values of unknown's constants mentioned in equations (25-25g) such as that flow and pressure gains can be calculated, as well as the losses that occur in transmission line.

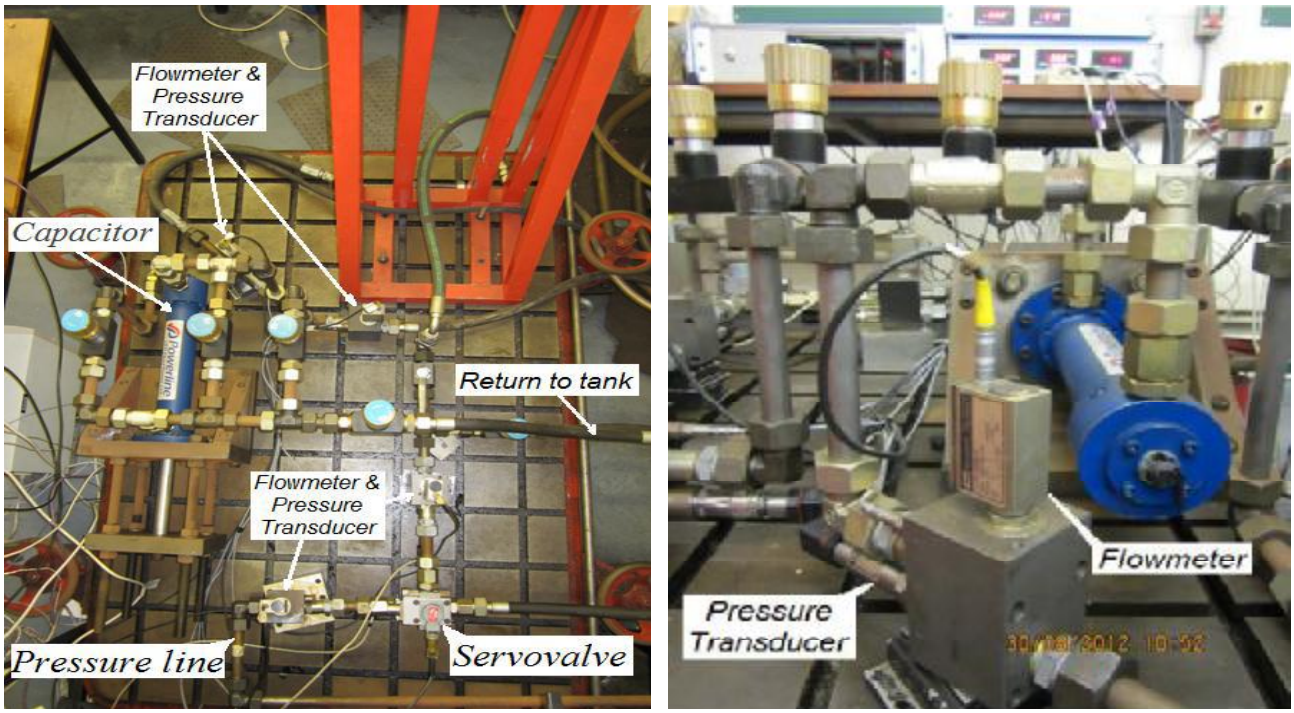


**(a) Top view for TL Test Rig.** **(b) Side view for TL Test Rig & Measurement Unite.**

**Fig. 7. Test Rig Transmission Line, Fluid Power Laboratory, W20/ School of Engineering / CARDIFF UNIVERSITY/ UK.**

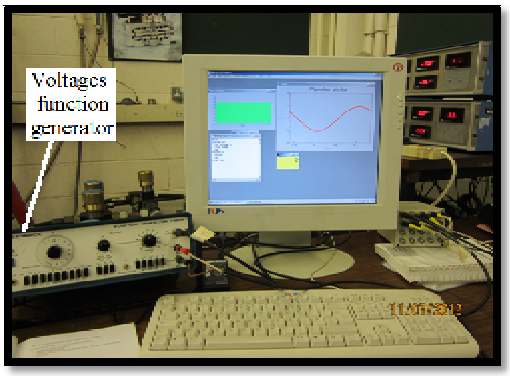


**Fig.8 Voltage Function Generato**

## 3. Experimental Approach

### 3.1. Modeling Assumptions

**Fluid properties**: As an initial condition, fluid properties will be; density of the hydraulic oil 860kg/m$^3$, absolute viscosity will be taken as 0.0258kg/m*s. Effective bulk modulus will be 1.5GN/m$^2$. Temperature effects are considered to be negligible, because the hydraulic system is supplied with a heat exchanger which maintains the hydraulic fluid temperature does not exceed 50$^o$C. Pressure variation effects are expected to be negligible, but will be investigated with respect to bulk modulus to confirm the system time-delay, a function of bulk modulus which is not affected. The bulk modulus is expected to be independent of pressure variation if there is considerable air in the system (either dissolved or as bubbles) so in this case there may be an effect.

**Transmission line dimensions**: TL consist of one 16m length of steel pipe the internal diameter is 12.5mm, wall thickness 2.3mm and with Young's modulus of 210GN/m$^2$ see Fig.7 (a).

**Pressure transducer:** (Parker- Sensor, type: SCP-150-1-06, 0-20 mA), shown in Fig.7 (b). The sensor response will be considered to be ideal, i.e. pure gain with no time delay. As investigated from (Hawkley), the transducer response has been considered an ideal sensor [11].

**Flow meter**: (Parker- Flow- sensor, type; SCQ-150-0-02, Range -150_+150 L/min, -3_+3 VDC), as illustrated in Fig. 7(b). The response will be considered accepted after subtracting the offset values at zero system pressure.

**The system has a continuous nature** The sample time must be kept to a minimum to avoid loss of dynamic characteristics. The DAP view cannot take more than 1Gbytes and the maximum voltage with applied to the servovalve is 10Volt.

**Transmission line termination** is assumed to be a simple (capacitor, resistance and inductance); the actuator cannot move (constant volume) as well the zero internal leakage is expected.

**Calibration of pressure transducer and DAP-card**, in all figures presented in this work, it presents a y-axis value of 'digital output' supplied from the pressure transducer to the DAP-card and saved in Excel-file. These values should be translated from digital voltage value to pressure value in bar. The digital sensor values are multiplied by (9.1*10$^{-3}$).

**Calibration of flow-meter and DAP-card,** to calibrate the flow rate in (L/min), the digital output from flow meters which collected by the DAP-card is needed to multiply by 15.26*10$^{-3}$.

### 3.2. Open Loop Pressure Control Results

Relying on the reference signal generator (Function generator) Fig. 8, The generated voltages are sent to the servovalve to change the system pressure in the chosen control point, and by using two types of waveforms, sinusoidal and square-wave. The voltages value was used in function generator ±4Volt. The delivery pressure line is set to be 50bar, noting that the highest values can DAP-card that gives it to the servovalve is 10*Volt*. The results are as shown in figures (Fig. 9, Fig.10 & Fig. 11). In these figures, the frequency values have been seized by using the voltages function generator as1*Hz***.**

### 3.3. Servovalve Transient Response

To find servovalve response and the amount of flow rate resulting from change voltage value, it is necessary to set up a special program using $C^{++}$ language in the *PC* and use the DAP-card ports to send the voltage signal to the servovalve amplifier card. This voltage signal energizes the servovalve torque motor to move the spool of the valve to build the pressure in transmission line. The $C^{++}$ program needs to change the voltage value gradually step by step at time interval of 2seconds to get a dynamic stability. This program starts from zero value to the highest value given by DAP-card (10*Volt*) and then back to a zero value. The stability can be observed in the flow rate in each step of the program as shown in Fig.12. After obtaining the flow values at each step, calculate the average flow rates in each step inside transmission line to find the relationship between voltage change and flow rate values changing. The flow rate measuring at point 2 (see Fig.1), represents the servovalve transient response output by the effect of the voltage input as illustrated in Fig.13.

### 3.4. The Transmission Line Losses and the Servovalve Gains

To find the properties of flow inside the transmission line, a steady state conditions has been create to record the values of pressure and flow rate inside the TL. By using these data, the servovalve gain could be found from the *Excel-file* that has been recorded by employing the

equations (25*b*, 25*d* & 25*f*). At 1.5 degree opening restrictor valve, the pressure inside the TL is accumulated. 50bar as a pressure line system is supply with a direct control using the voltages function generator. The results are coming from the square-wave voltage illustrated in Fig. 14 & Fig. 15.

Through the act of the experimental test, the nature of the flow rate has been checked as a laminar flow by calculating the Reynolds number and the velocity from recorded flow. The relation between the voltage and the spool position inside the servovalve has been found from Bode diagram supported by manufacturer data sheet, see {Appendix-A}.

The fluid power unit of the laboratory supplies many test rigs. So it was difficult to find out the miner losses through the line supply the test bench which have been used as well as the fluctuation effect. The minor losses mean the pressure drop due to elbows, junction, reducers, valves and hoses…etc. The major losses occurring in TL can be calculated from the equation below [12]:

$$\Delta P_{majer} = 4f(\rho * U_3^2)\left(\frac{L_{TL}}{d_{i3}}\right), \quad where: U_3 = \frac{Q_3}{a_3} \qquad \ldots(28a)$$

An experimental test have been used to find the total losses ( $\Delta P_{Total}$) between point 2 & 3 as located in Fig. 1, where:

$$\Delta P_{Total} = \Delta P_{majer} + \Delta P_{minor} \qquad \ldots(28b)$$

Then:

$$\Delta P_{minor} = 4f(\rho * U_3^2)\left(\frac{L_{equiv}}{d_{i3}}\right) \qquad \ldots(28c)$$

So the *equivalent length* $L_{equiv}$ = 18.46*m*, and the corrected total TL length become:

$$L_c = L_{TL} + L_{equiv} \qquad \ldots(28d)$$

The total corrected length ($L_c$=*l*) has been used in equations (26d) to solve the mathematical model.

### 3.5. MATLAB Simulation and Results

To find a mathematical model for the TL equations (27a and 27b) and the servovalve flow rate equations (24) supported by the voltage linearization equations (25*b*, 25*d* & 25*f*) that mentioned before, MATLAB *m-file* program can be used to represent the transmission line effect after converting to electric analogy.

There has been a great complexity of the hydraulics system in the fluid power laboratories in Cardiff University and the large size of the power unit system as well as the length of the pipes connected with TL test rig. Besides, the hydraulic pressure provided for two laboratories and several hydraulic apparatus are connected to them. For this reasons, some assumptions have been taken in to account such as: the pressure provided by the supplied pressure line which delivers the fluid to the servovalve was considered as constant pressure in MATLAB program. This will neglect the fluctuation of the pressure value caused by system complexity.

To find a clear comparison between the selected practical experiences and the program built by using MATLAB *m-file*, it is essential to find the values for the gain needed. The sample was taken from the recorded data, which represent a step input supplied by the function generator and compared to the output values resulting from the MATLAB *m-file* designed program. As shown in figures (Fig. 16a & Fig. 16b) and (Fig. 16c & Fig. 16d), the consequence output values are compatible in the behavior as well as the value. The exceptions of that compatibility seen in the overshot behavior can be explained by the pressure input values in the instant of the step input. The pressure input value to the servovalve is decreased in the instant of the step input while the pressure input value in MATLAB program maintains in constant value. The result predicted from MATLAB *m-file* program shows the pressure values variation in the effect of servovalve opining and the TL delay effect as illustrated in Fig.16b.

The noise and oscillations shown in Fig 15 and Fig.16c, for the values of flow rate result from the nature of flow meter design. As mentioned previously there is an error should be dealt with and reduced by subtracting the offset value and depending on the average values to solve the mathematical equations.

The MATLAB *m-file* program can create a various shape of input voltage value (sine-wave or square-wave). The pressure and flow rate output could be seen for square wave in Fig. 17a & Fig17b. The behaviors of the mathematical model have a good approach comparing to the experimental test seen in Fig. 14 & Fig.15. The sine-wave input voltages generated in *m-file* program are supplied to the servovalve, the pressure and flow rate output shown in Fig.18a & Fig. 18b. It is clear that there is a delay effect of the TL especially in pressure output as seen in Fig. 18a.

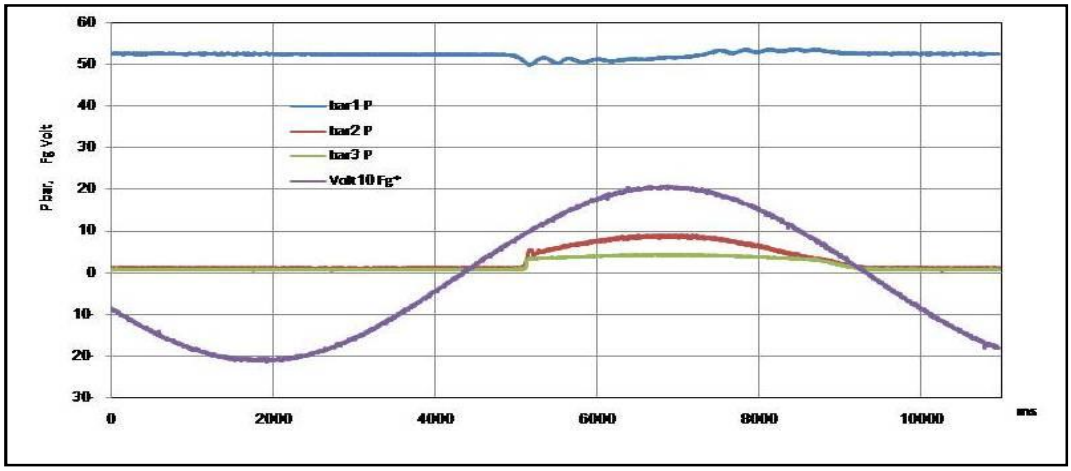


**Fig. 9. Open Loop Controlled by Voltage Function Generator Ps=52bar with sin-wave voltage Amplitude Fg=4volt.**

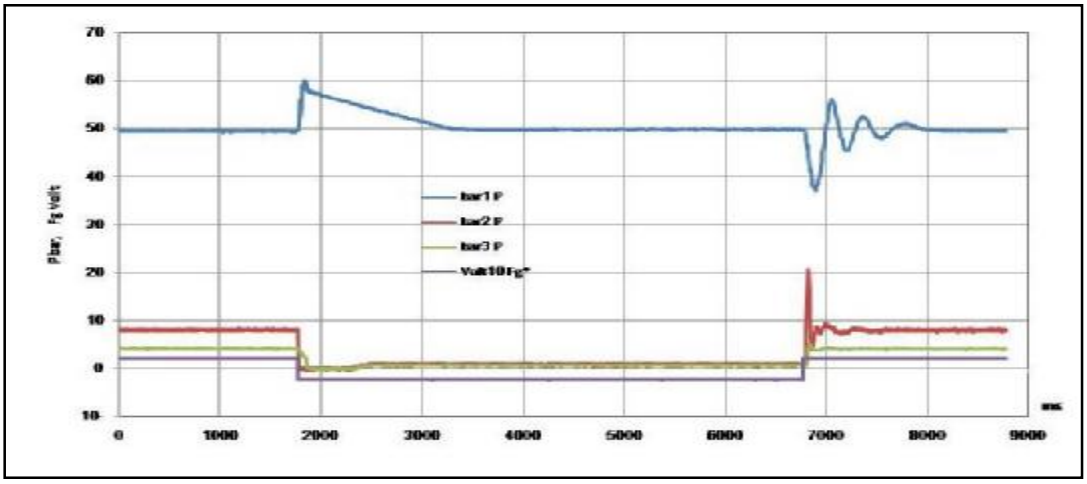


**Fig. 10. Open Loop Controlled by Voltage Function Generator Ps=50bar with Square-Wave Voltage Amplitude Fg=4volt.**

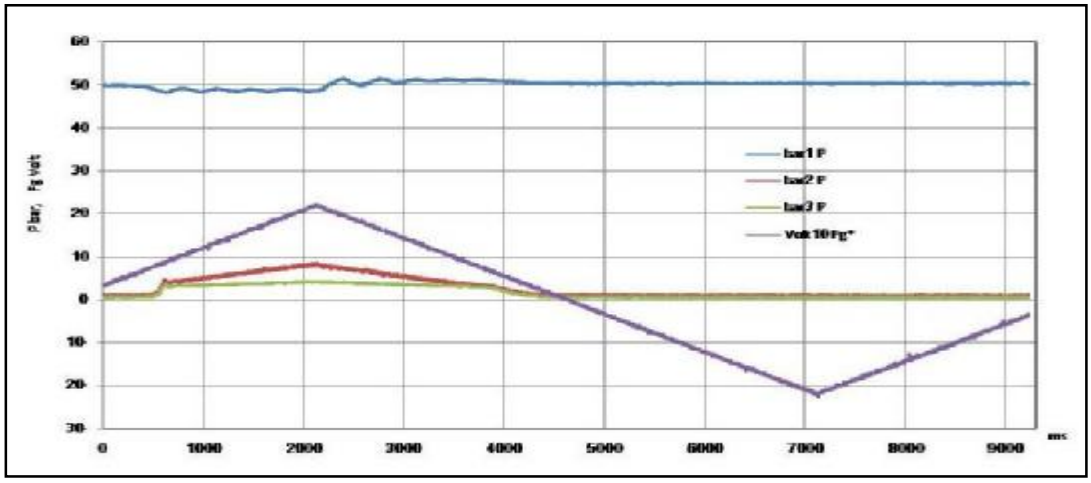


**Fig. 11. Open Loop Controlled by Voltage Function Generator Ps=50bar with Saw-Wave Voltage Amplitude Fg=4volt.**

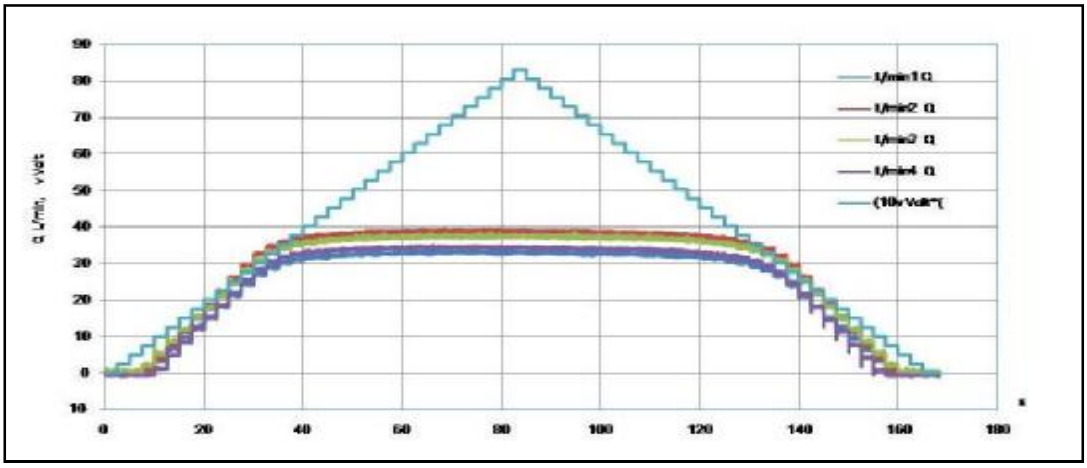

**Fig. 12. Flow Rate and Servovalve Voltage Data Variation In Transmission Line at Ps=70 bar.**

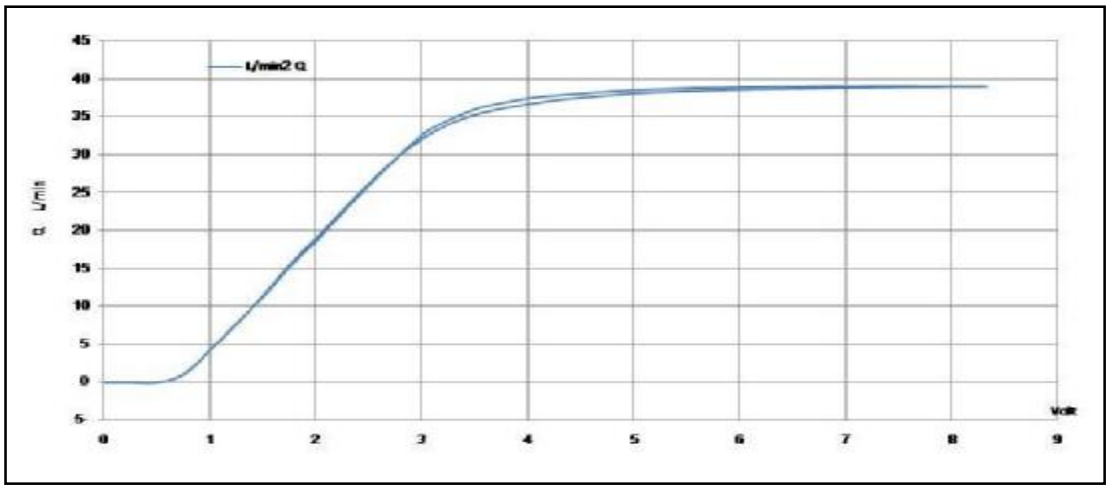


**Fig. 13. Transient Responses of Servovalve.**

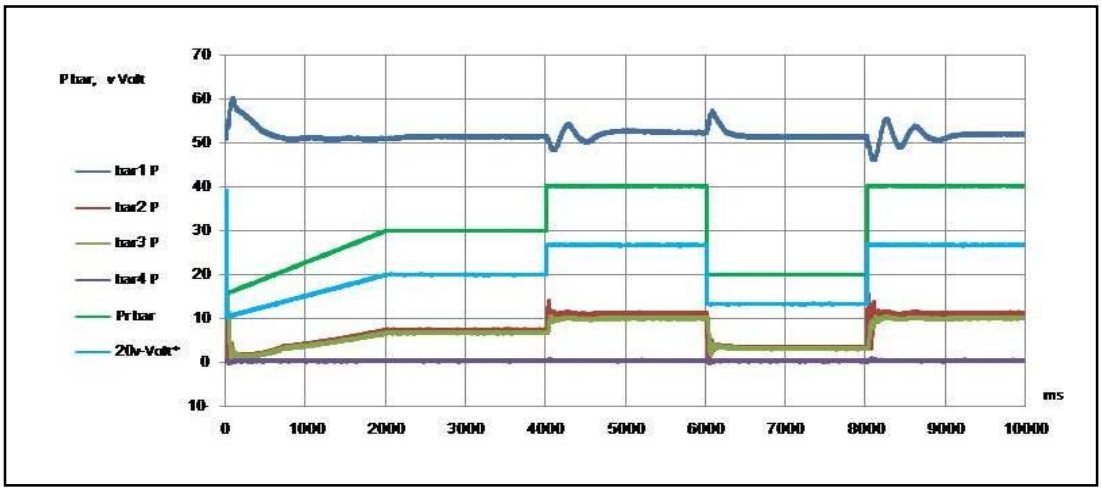


**Fig. 14. Open Loop Controlled by C++ Program (1.5 Degree Opening from the Restrictor Valve), Square-Wave, P1=50bar, Fr=0.25Hz.**

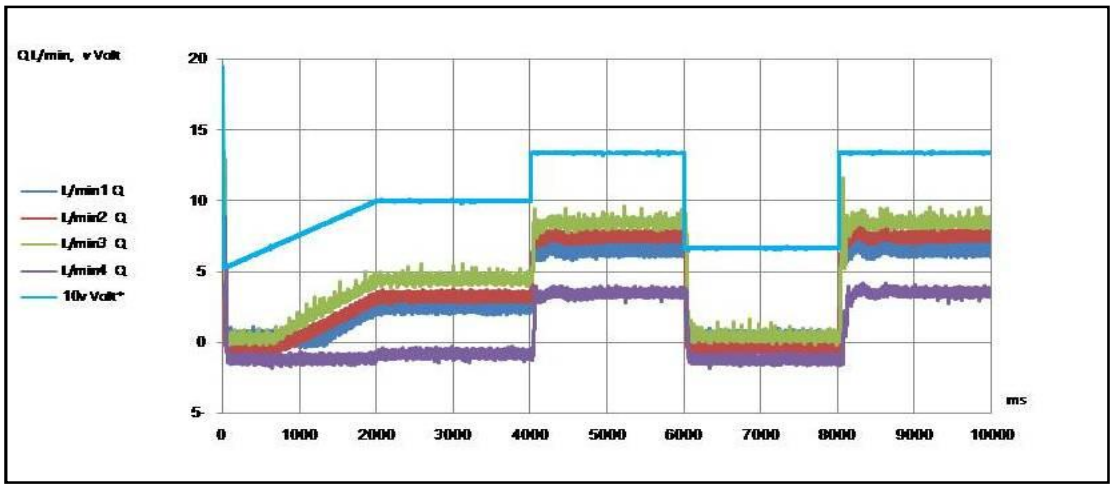


**Fig. 15. Open Loop Controlled by C++ Program (1.5 Degree Opening from the Restrictor Valve), Square-Wave, P1=50bar, Fr=0.25Hz.**

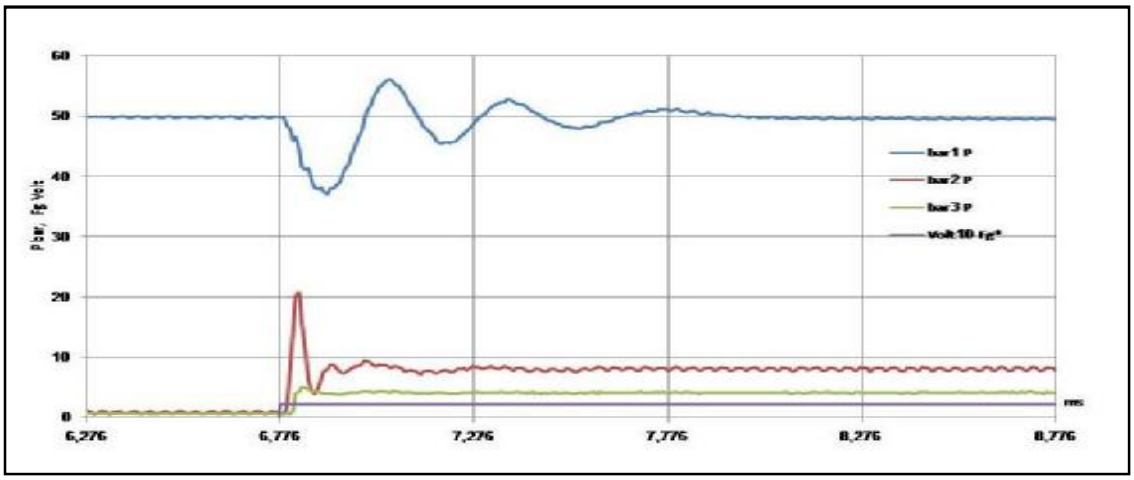


**Fig. 16a. Open Loop Controlled by Voltage Function Generator P1=50bar, Time Sampling = 8ms.**

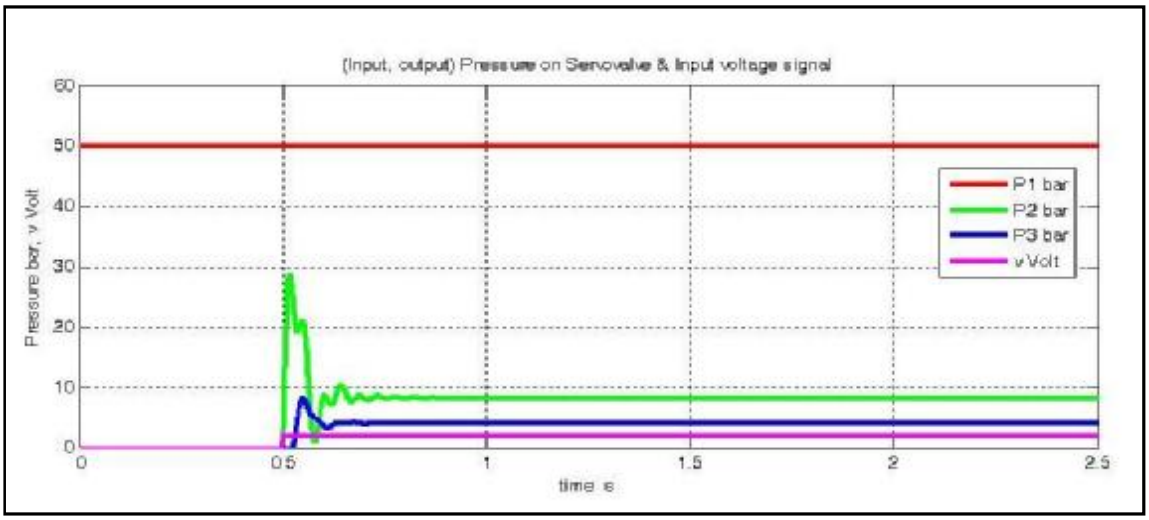


**Fig. 16b. Open Loop Controlled by MATLAB m-file P1=50bar, Time Sampling = 1ms.**

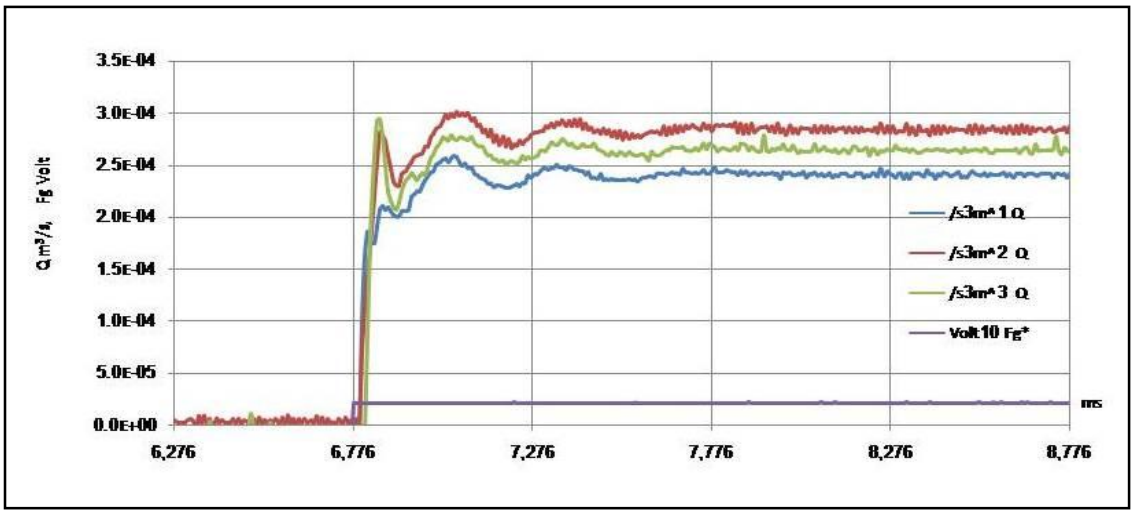


**Fig. 16c. The Flow Rate in Open Loop Controlled by Voltage Function Generator P1=50bar, Time= 2.5 s.**

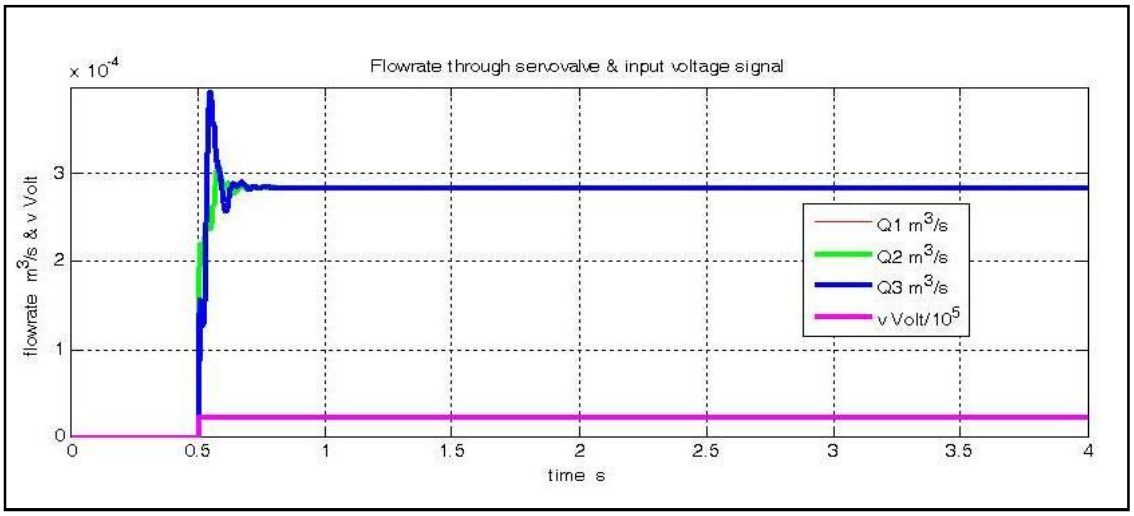


**Fig. 16d. The Flow Rate in Open Loop Controlled by MATLAB m-file P1=50bar, Time= 2.5 s.**

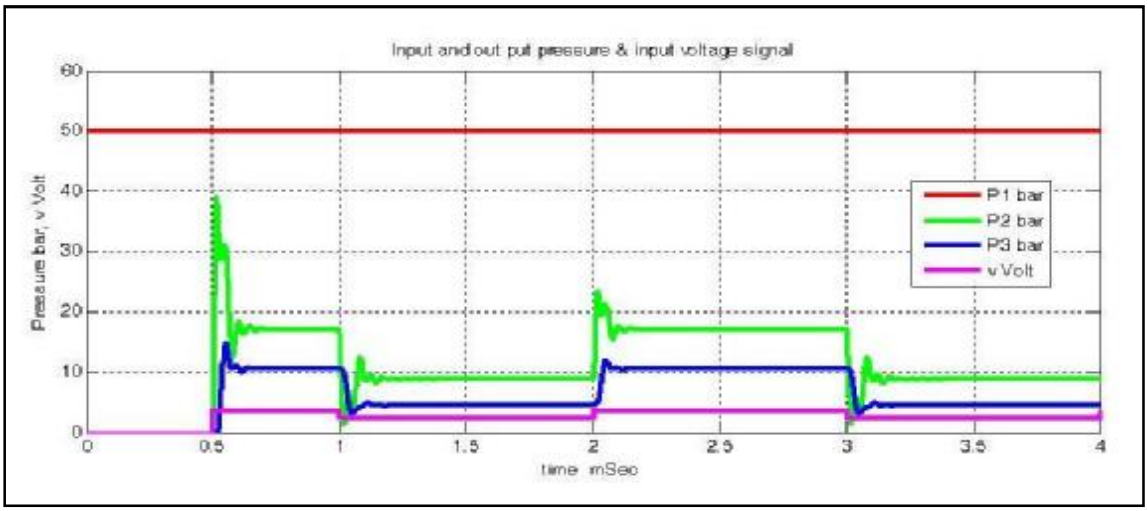


**Fig. 17a. The Pressure Values in Open Loop Servovalve Controlled, by MATLAB m-file P1=50bar, Square Wave, Time= 4.0s.**

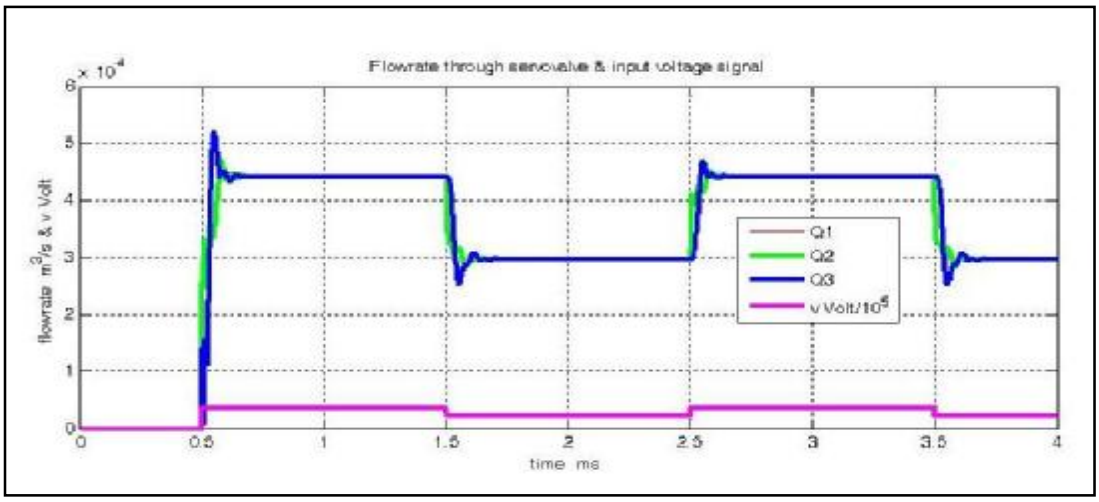


**Fig. 17b. The Flow Rate Values in Open Loop Servovalve Controlled, by MATLAB m-file P1=50bar, Square Wave, Time= 4.0s**

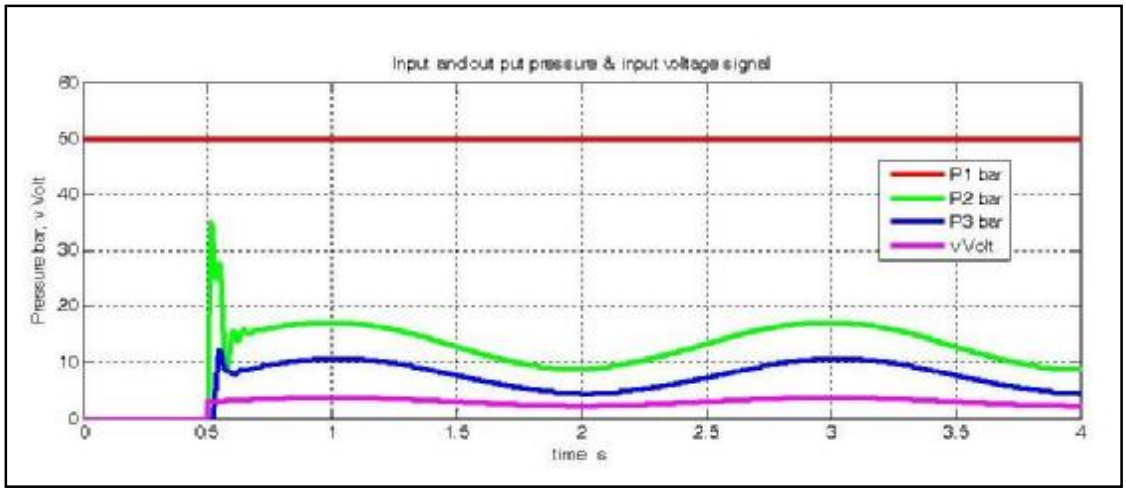


**Fig. 18a. The Pressure Values in Open Loop Servovalve Controlled, by MATLAB m-file P1=50bar, Sine Wave, Time= 4.0s.**

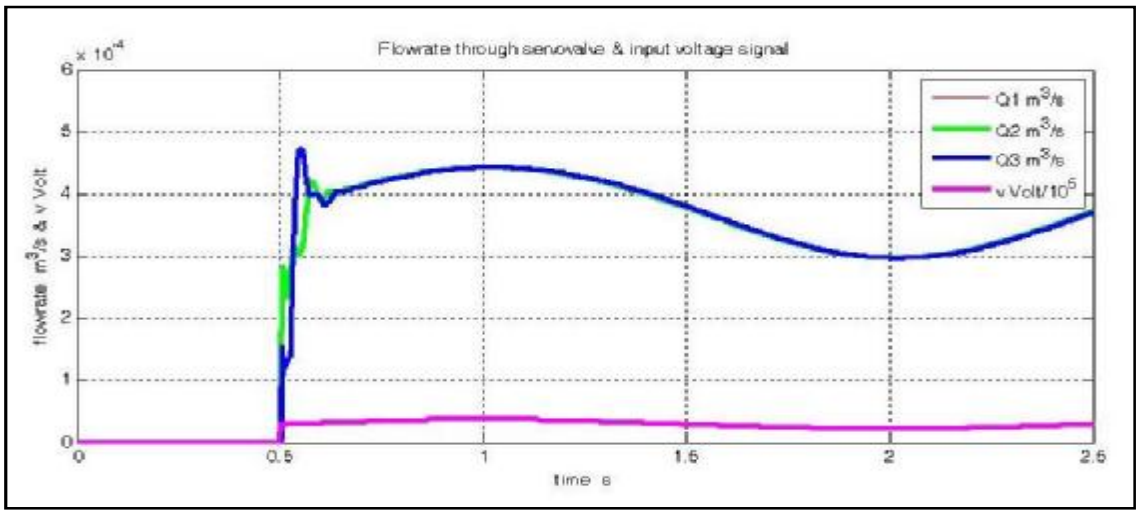


**Fig. 18b. The Flow Rate Values in Open Loop Servovalve Controlled, by MATLAB m-file P1=50bar, Sine Wave, Time= 4.0s.**

## 4. Conclusions

Foregoing became clear that the use of the open loop control study is very important to know the properties of the system and its capabilities. The open loop concept is the first step to entrance and design the efficient closed loop control to attenuate the delay TL effect.

The servovalve (mechanical feedback) is one of the efficient valves that can be used to control the specific pressure value on the actuator. To reduce the impact of losses resulting from the hydraulic flow rate inside a long TL, the closed loop concept should be used.

The lumped π element electrical analogy method for laminar flow is an efficient method which simulates the TL module. The relation between the flow rate and the supplied voltage of the servovalve amplifier is almost a linear relation one and the effect of design complexity could be neglected. This concept is so clear in the transient response of the electro-hydraulic servovalve.

Found through experimental tests that the value of the time sampling recorded through a DAP-view program could be taken as *1* millisecond and that provided a good accurate data that can be used to calculate the simulation system in MATLAB m-file program. The DAP-view program is used to control the servovalve and it shows a precise action and follows the program designed in $C^{++}$ formula with different shape of functions.

## Nomenclature

### Latin Characters

| Character | Description | Units |
|---|---|---|
| $a$ | Hydraulic pipeline cross section area | $m^2$ |
| $a_n$, $a_{nx}$, $a_{ny}$ | Nozzle cross section area | $m^2$ |
| $a_n$ | The nozzle area | $m^2$ |
| $a_s$ | The spool cross section area | $m^2$ |
| $a_o$ | The spool orifice area | $m^2$ |
| $B_v$ | The fluid viscous coefficient | $m^2$ |
| $C_q$, $C_{qn}$, $C_{qo}$ | The flow coefficients of the orifices and the nozzles | - |
| $C$ | Electrical capacitance | Farad |
| $d_i$ | Pipe ( Transmission line) internal diameter | m |
| $d_n$ | The nozzle diameter | m |
| $d_o$ | The orifice diameter | m |
| $E_i$ | Electrical inductance | |
| $F$ | Frequency | Hz |
| $Fg$ | Voltage input from the Voltage Function Generator | Volt |
| $f$ | Darcy friction factor | - |
| $Q_1$, $Q_2$ | Flow rate from servovalve | $m^3/s$, $l$/min |
| $Q_a$, $Q_b$ | The orifice discharge | $m^3/s$ |
| $Q_x$, $Q_y$ | The nozzle discharge | $m^3/s$ |
| $i$ | The input torque motor current | mA |
| $I$ | Current | A |
| $\Delta i$ | Input differential current | mA |
| $J$ | The flapper inertia | kgm/s |
| $P_a$, $P_b$ | Pressure at nozzle *a* and nozzle *b* | $N/m^2$ |
| $P_{Load}$ | The pressure difference on the load | $N/m^2$ |
| $P_s$ | System pressure | $N/m^2$; bar |
| $k_a$ | Flexure tube rotational stiffness | Nm/rad |
| $k_c$ | Servovalve constant | |
| $k_f$ | The cantilever springs stiffness | Nm/rad |
| $k_{fr}$ | The flow reaction equivalent stiffness | |
| $k_m$ | Electromagnetic spring constant of torque motor | Nm/rad |
| $k_t$ | Electromagnetic constant of torque motor | Nm/Amp |
| $l$ | Hydraulic pipeline length | m |
| $L$ | Electrical inductance | Henry |
| $L_c$ | Corrected length | m |
| $L_{equiv}$ | Equivalent losses length | m |
| $L_{TL}$ | Transmission line length | m |
| $R$ | Electrical resistance | Ω |
| $r$ | The distance between the nozzle center line and flexure joint | m |
| $T$ | The torque on the flexure tube | N.m |
| $T_f$ | The resisting torque | N.m |
| $U$ | The spool velocity | m/s |
| $U_3$ | The output mean flow rate velocity from the servovalve | m/s |
| $u$ | Control signal | volt |
| $V$ | Volume | $m^3$ |
| $V_e$ | Electrical Voltage | volt |
| $v$ | input voltage | volt |
| $w$ | The rectangular port area gradient | m |

| | | |
|---|---|---|
| $x$ | The displacement of the flapper at the nozzles | m |
| $x_s$ | The spool displacement | m |
| $x_{nm}$ | Flapper clearance in the mid position | |
| $y$ | Total spring deflection | m |
| $Z$ | Constant for the servovalve design parameter (valve characteristic) | |

## Greek Symbols

| Character | Description | Units |
|---|---|---|
| $\beta$ | Effective Bulk modulus | $N/m^2$ |
| $\mu$ | Fluid absolute viscosity | kg/m.s |
| $\rho$ | Fluid density | $kg/m^3$ |
| $\theta$ | The rotation of the armature and flapper | rad |

## subscripts

| | | |
|---|---|---|
| *ss* | Steady state operation condition | - |
| | | - |

## 5. References


[1] DSP Control of Electro-Hydraulic Servo Actuators (January 2005), Application Report, Texas Instruments SPRAA76.

[2] Le Bon. A. & Hug, P. (1996), "Book of steel, "The manufacture of plain carbon sheet steels - reheating and hot rolling", Lavoisier publishing.

[3] Watton, J., & Hawkley, C. J. (1996). An approach for the synthesis of oil hydraulic transmission line dynamics utilizing in situ measurements. Proceedings of the Institution of Mechanical Engineers, Journal of Systems and Control Engineering, Part I, 77-93.

[4] Krus, P. &. (2000). COMPLETE AIRCRAFT SYSTEM SIMULATION FOR AIRCRAFT DESIGN PARADIGMS FOR MODELLING OF COMPLEX SYSTEM. ICAS 2000 CONGRESS (pp. 613.1-613.9). Sweden: Department of Mechanical Engineering, Linköping University.

[5] Dong, C., Zhu, Y., & Lu, J. (2010). Modeling and dynamic behavior analysis of a hydraulic servo system with consideration of pipeline effect. International Conference of Logistics Engineering and Management: Logistics for Sustained Economic Development - Infrastructure, Information, Integration (pp. 3153-3160). Harbin, China: College of Engineering and Technology, Northeast Forestry University.

[6] Yang, L. & Moan, T. (2011). Dynamic analysis of wave energy converter by incorporating the effect of hydraulic transmission lines. Ocean Engineering, Elsevier, Vol. 38, pp. 1849-1860.

[7] DAP-view user manual, Microstar labs, 2001.

[8] Cundiff, J. S. (2002). Fluid Power Circuits and Controls: fundamentals and applications. Library of Congress Cataloging-in-Publication: (Mechanical engineering series), TJ840.C85 2001, 621.2—dc21.

[9] Watton, J. (1989). Fluid power systems, Modeling, simulation, analog and microcomputer control. UK: Prentice Hall.

[10] Watton, J. (2009). *Fundamentals of Fluid Power Conntrol.* CAMBRIDGE/UK: CAMBRIDGE UNIVERSITY PRESS.

[11] Hawkley, C. J. (1996). The modelling and simulation of an electrohydraulic pressure control system.PhD, thesis. UK: School of Engineering, UWCC, Cardiff University.

[12] Frank M. White (2005), Fluid Mechanics Fourth Edition, University of Rhode Island McGraw-Hill Series in Mechanical Engineering.

Appendix –A: PERFORMANCE DATA~4551, 4592, 4657, 4658 SERIES VALVE (Moog).

## PERFORMANCE DATA - 4551, 4592, 4657, 4658 SERIES VALVE

Figure 1 Flow Characteristics

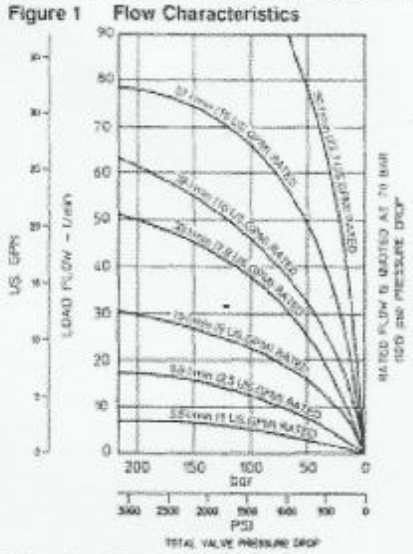

Figure 2 Typical Flow Gain

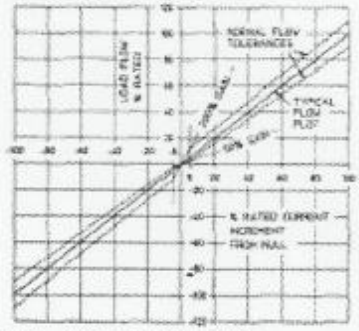

Figure 3 Transient Response

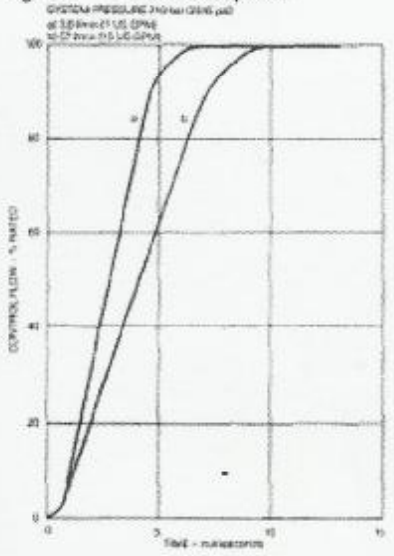

Figure 4 Dynamic Response

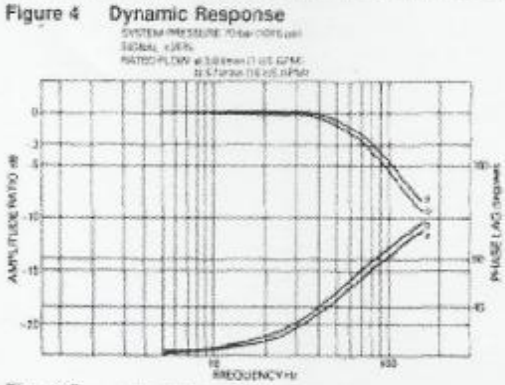

Figure 5

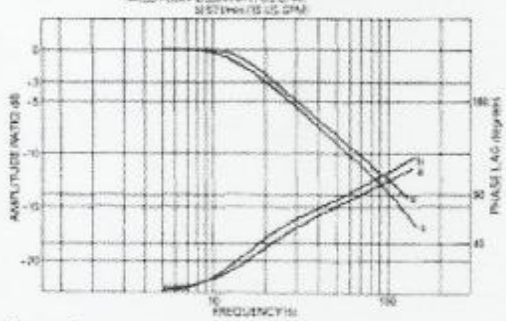

Figure 6

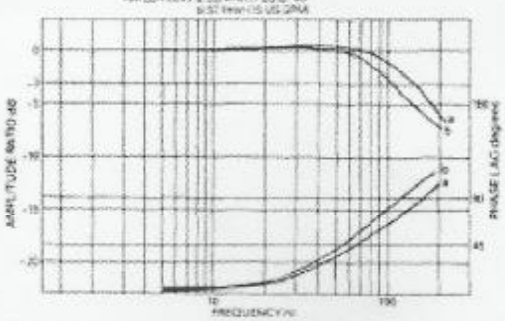

Figure 7

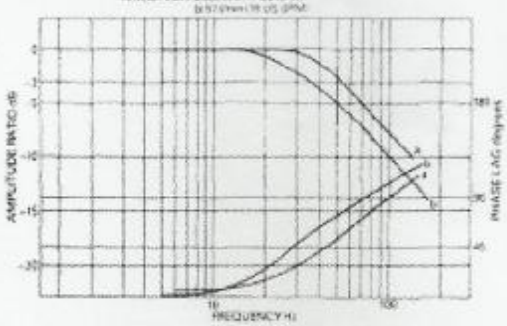

# السيطرة على الضغط باستخدام الصمام الموازر الكهروهيدروليكي وتاثير الخط الناقل للهيدروليك

**جعفر مهدي حسان* يكن اكسو** ماجد احمد عليوي*****

**احمد فؤاد مهدي******

*قسم الهندسة الميكانيكية / الجامعة التكنولوجية

**كلية الهندسة / جامعة كاردف- بريطانيا

***قسم هندسة السيطرة والنظم / الجامعة التكنولوجية

****قسم هندسة التصنيع المؤتمت / كلية الهندسة الخوارزمي

*البريد الالكتروني: JafarMahdi1951@yahoo.com

**البريد الالكتروني: xue@cf.ac.uk

***البريد الالكتروني: moleiwi@yahoo.com

****البريد الالكتروني:afmkridi@hotmail.com

**الخلاصة**

في بعض الحالات يعتبر الخط الناقل للهيدروليك بين المستهلك (المحرك) و صمام السيطرة مهم ومؤثر. هذه الدراسة تركز على نمذجة الخط الناقل للهيدروليك الواصل بين صمام السيطرة الموازر الكهروهيدروليكي والمستهلك. تمت السيطرة على قيمة الضغط داخل الخط الناقل من خلال السيطرة على قيمة الفولتية الواصلة الى المضخم الخاص بصمام الموازر. تمت نمذجة الجريان الطباقي داخل الخط الناقل باستخدام طريقة $\pi$ للكم لتحويل الخط الناقل الى منظومة كهربائية. تم استخدام الطريقة المباشرة في التحكم بالفولتية من خلال جهاز مولد دالة الفولتية وبشكل غير مباشر من خلال استخدام برامج ال ($C^{++}$) والذي يرتبط مع برنامج (DAP-view) المنصب اصلا في الدائرة الكهربائية (DAP-card) التي يمكن أضافتها الى الكومبيوترات الشخصية للسيطرة على قيمة الضغط داخل الخط الناقل عند نقطة معينة مختارة. تم التوصل الى ان العلاقة بين الفولتية والجريان الخارج من صمام الموازر في اغلب الاحيان علاقة خطية. تم استخدام برنامج الماتلاب (*m-file*) لايجاد حالة تمثيل رياضي و وجد بأن النتائج كانت جيدة لحالة السيطرة على الدائرة المفتوحة ومتماثل مع التجارب العملية.